Chapter 2

Acoustic Wave Velocity Measurement on Piezoelectric Ceramics

Toshio Ogawa

Additional information is available at the end of the chapter

http://dx.doi.org/10.5772/53117

1. Introduction

1.1. Why is "acoustic wave velocity measurement" needed?

1.1.1. Relationships between Young's modulus and electromechanical coupling factor in piezoelectric ceramics and single crystals

Material research on lead-free piezoelectric ceramics has received much attention because of global environmental considerations. The key practical issue is the difficulty in realizing excellent piezoelectricity, such as electromechanical coupling factors and piezoelectric strain constants, by comparison with lead zirconate titanate [$Pb(Zr,Ti)O_3$] ceramics. The coupling factor is closely related to the degree of ferroelectric-domain alignment in the DC poling process. We have already shown the mechanism of domain alignment in $Pb(Zr,Ti)O_3$ (PZT) [1-5], $PbTiO_3$ (PT) [6], and $BaTiO_3$ (BT) [7] ceramics and in relaxor single crystals of $Pb[(Zn_{1/3}Nb_{2/3})_{0.91}Ti_{0.09}]O_3$ (PZNT91/09) [8] and $Pb[(Mg_{1/3}Nb_{2/3})_{0.74}Ti_{0.26}]O_3$ (PMNT74/26) [9] by measuring the piezoelectricity vs DC poling field characteristics. Throughout the studies, we have discovered relatively high coupling factor of transverse vibration mode k_{31} over 80 % (it called giant k_{31}) in the relaxor single-crystal plates [10,11]. Furthermore, we reported that the origin of giant k_{31} is due to the lowest Young's modulus of the single-crystal plates [11,12]. The results indicate the important relationships between Young's modulus and electromechanical coupling factor to realize high piezoelectricity.

Concrete experimental results are mentioned as follows. The Young's modulus (Y^E) of PZNT91/09 single crystals with giant k_{31} (Y^E=0.89x10^{10} N/m^2) is one order of magnitude smaller than the Y^E (6~9x10^{10} N/m^2) of PZT ceramics, and roughly speaking, one order of magnitude larger than the Y^E (0.05x10^{10} N/m^2) of rubber [12]. It was thought that the origin

of giant k_{31} in PZNT91/09 and PMNT74/26 single crystals was due to the mechanical softness of the materials. Namely, the most important factor to realize high piezoelectricity is easy deformation by the DC poling field. Figure 1 shows the relationships with k_{31} and k_{33} (a coupling factor of longitudinal vibration mode) vs Y^E on various kinds of single crystals and ceramics reported [13]. There is a linear relationship with k_{31} vs Y^E and k_{33} vs Y^E. Furthermore, there is a blank space between Y^E of PZNT91/09 and PMNT74/26 single crystals and Y^E of ordinary piezoelectric materials. Therefore, the important viewpoint is that new piezoelectric materials including lead-free compositions with higher coupling factor should be investigated to clarify the blank space, such as the research for elements softened the materials in lead-free ceramics.

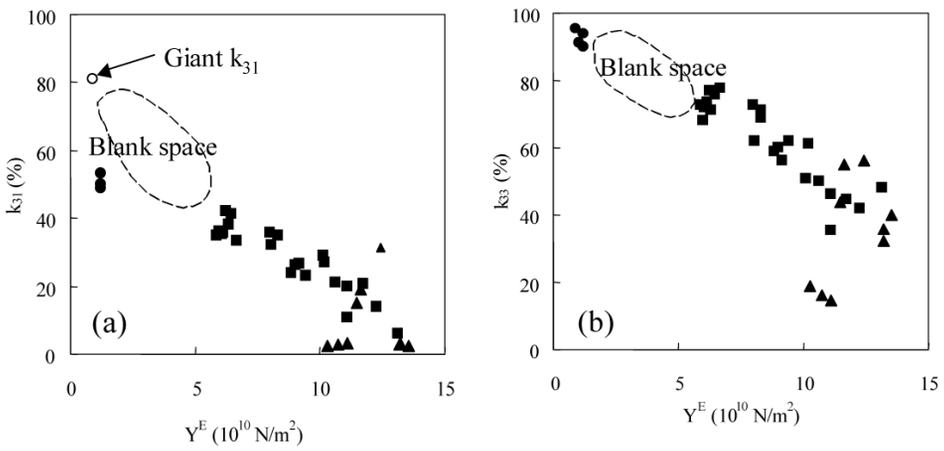

Figure 1. Relationships with coupling factors of (a) k_{31} and (b) k_{33} vs Young's modulus (Y^E) in piezoelectric materials.

1.1.2. Newly developed measurement method for acoustic wave velocities

Elastic constants of piezoelectric ceramics such as Young's modulus and Passion's ratio were basically evaluated by impedance responses on frequency of piezoelectric resonators with various relationships between DC poling directions and vibration modes [14-17]. Therefore, it needs all kinds of resonators with different shapes [14], and furthermore, with uniform poling-degree in spite of different poling-thicknesses such as 1.0 mm for plate resonators (for example, dimensions of 12 mm length, 3.0 mm width and 1.0 mm poling-thickness) and 15 mm for rod resonators (dimensions of 6.0 mm diameter and 15 mm poling-thickness). While applying a DC poling field of 3.0 kV/mm, 3.0 kV DC voltage must be applied to the former sample and 45 kV for the later sample. There was no guarantee to obtain uniform poling-degree between two samples even through the same poling field of 3.0 kV/mm. In addition, it is difficult to measure in the cases of as-fired ceramics, namely ceramics before poling, or weak polarized ceramics because of none or weak impedance responses on frequency.

On the other hand, there was a well-known method to measure the elastic constants by pulse echo measurement [18,19]. Acoustic wave velocities in ceramics were directly measured by this method. However, since the frequency of pulse oscillation for measurement

http://dx.doi.org/10.5772/53117

was generally below 5 MHZ, it needs to prepare the rod samples with thickness of 10-20 mm in order to guarantee accuracy of the velocities. Moreover, it is unsuitable for measuring samples such as disks with ordinary dimensions (10-15 mm diameter and 1.0-1.5 mm thickness) and with many different compositions for piezoelectric materials R & D.

We developed a method to be easy to measure acoustic wave velocities suitable for the above mentioned disk samples by an ultrasonic thickness gauge with high-frequency pulse oscillation. This method was applied to hard and soft PZT [3], lead titanate [6] (both lead-containing ceramics) and lead-free ceramics composed of alkali niobate [20,21] and alkali bismuth titanate [22]. In this chapter, first of all, we report on the measurement of acoustic wave velocities in PZT ceramics, and the following, the calculation results of Young's modulus and Poisson's ratio, especially to obtain high piezoelectricity in lead-free ceramics.

For the measurement, the ultrasonic precision thickness gauge (Olympus Co., Model 35DL) has PZT transducers with 30 MHz for longitudinal-wave generation and 20 MHz for transverse-wave generation. The acoustic wave velocities were evaluated by the propagation time between second pulse echoes in thickness of ceramic disks with dimensions of 14 mm in diameter and 0.5-1.5 mm in thickness. The sample thickness was measured by a precision micrometer (Mitutoyo Co., Model MDE-25PJ). Piezoelectric ceramic compositions measured were as follows: $0.05Pb(Sn_{0.5}Sb_{0.5})O_3$-$(0.95-x)PbTiO_3$-$xPbZrO_3$ (x=0.33, 0.45, 0.48, 0.66, 0.75) with (hard PZT) and without 0.4 wt% MnO_2 (soft PZT) [3]; $(1-x)(Na,K,Li,Ba)(Nb_{0.9}Ta_{0.1})O_3$-$xSrZrO_3$(SZ) (x=0, 0.02, 0.04, 0.05, 0.06, 0.07) [20,21]; $(1-x)(Na_{0.5}Bi_{0.5})TiO_3$(NBT)-$x(K_{0.5}Bi_{0.5})TiO_3$ (KBT) (x=0.08, 0.11, 0.15, 0.18, 0.21, 0.28) and $0.79NBT-0.20KBT-0.01Bi(Fe_{0.5}Ti_{10.5})O_3$(BFT) [22]; and $(1-x)NBT-xBaTiO_3$(BT) (x=0.03, 0.07, 0.11) [22]. In addition to evaluate ceramic compositions, we investigated ceramics with different ceramic manufacturing processes such as firing processes of normal firing in air atmosphere and oxygen atmosphere firing to realize pore-free ceramics [23], and DC poling processes of as-fired (before poling), weakly and fully polarized ceramics.

2. Young's modulus and Poisson's ratio in piezoelectric ceramics

2.1. Longitudinal and transverse wave velocities by pulse echo measurement

Figure 2 shows pulse echoes of longitudinal acoustic wave in hard PZT ceramics at a composition of x=0.48. The longitudinal wave velocity was calculated from the propagation time between second-pulse echoes (␣) and the thickness of ceramic disks. The dependences of the longitudinal and transverse wave velocities on the composition of x in hard and soft PZT ceramics and their fluctuation of the individual ceramic disks were shown in Figs. 3(a)-(d). The fluctuation of the velocities in transverse wave was smaller than the ones in longitudinal wave when the samples of n=16-21 pieces were measured at each composition. In addition, it was clarified that the fluctuation in soft PZT was smaller than the one in hard PZT ceramics because of easy alignment of ferroelectric domains by poling field in soft PZT, namely lower coercive fields than the ones of hard PZT.

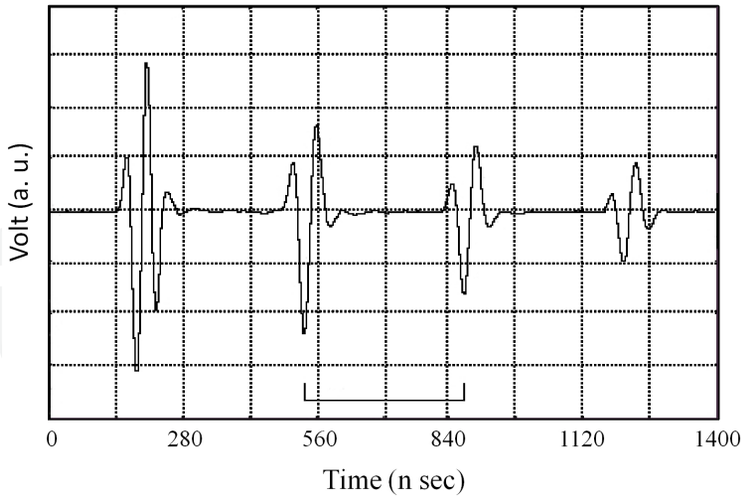

Figure 2. Pulse echoes of longitudinal acoustic wave in hard PZT ceramics (disk dimensions: 13.66 mm diameter and 0.735 mm thickness) before poling at x=0.48; the calculated wave velocity is 4,319 m/s.

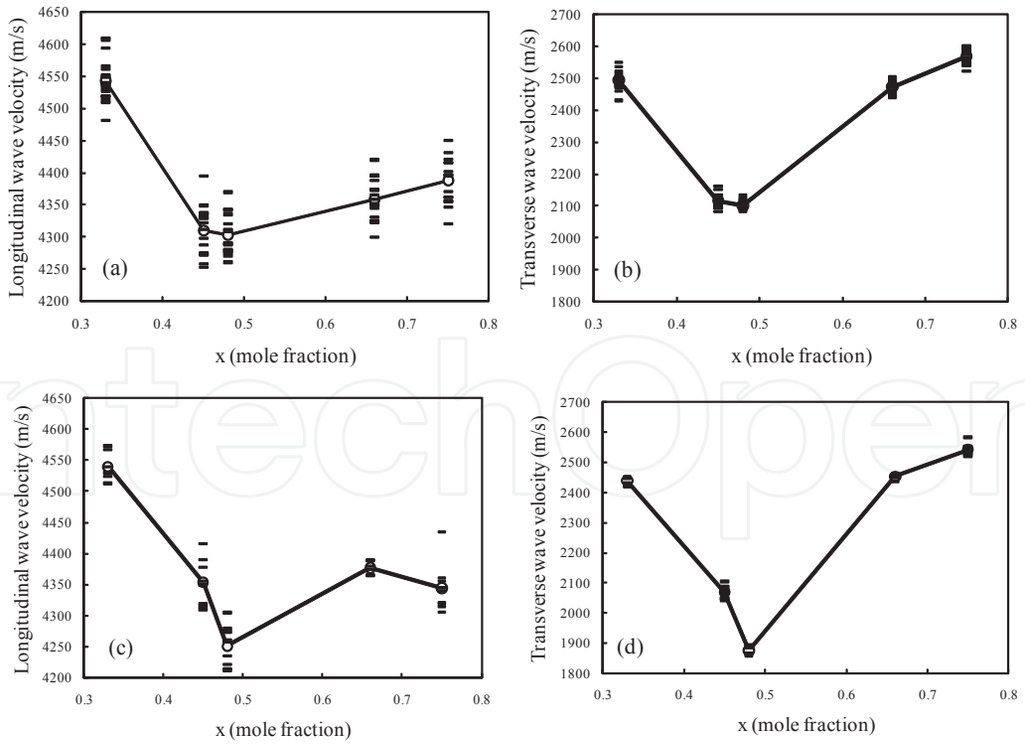

Figure 3. Composition x dependence of longitudinal and transverse wave velocities in hard [(a) and (b)] and soft PZT [(c) and (d)] ceramics before poling; all the samples of n=16-21 are shown in the figure to evaluate their fluctuation.

2.2. Young's modulus and Poisson's ratio in PZT ceramics

Figures 4(a)-(d) show the dependences of the longitudinal and transverse wave velocities, Young's modulus and Poisson's ratio on the composition of x in hard and soft PZT ceramics, respectively. Here, the elastic constants were calculated from equations in the following session 3.1. From Fig. 4, it was found that the large differences in these values between hard and soft PZT ceramics only occurred around a composition of x=0.48, which corresponds to a morphotropic phase boundary (MPB) [23].

In the case of the evaluation on ceramic manufacturing processes, the values of pore-free ceramics fired in oxygen atmosphere also show in the figures at compositions of x=0.66 and 0.75 (in dotted circles, the samples of n=2). The effect of reducing pores in ceramics on the values works like the increase of the longitudinal wave velocity and Poisson's ratio, and the decrease of the transverse wave velocity and Young's modulus.

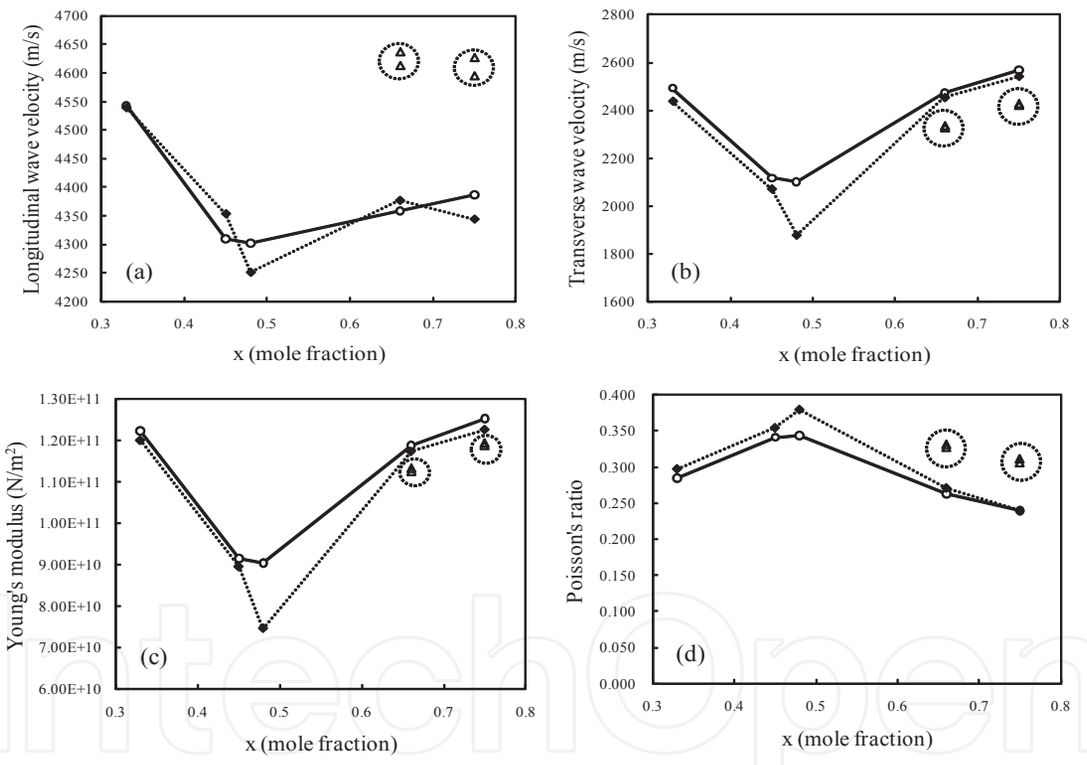

Figure 4. Composition x dependence of (a) longitudinal and (b) transverse wave velocities, (c) Young's modulus and (d) Poisson's ratio in hard (—) and soft (---) PZT ceramics before poling; the values of pore-free hard PZT ceramics (x=0.66, 0.75 and the samples of n=2) were shown in dotted circles.

As mentioned later in the session 4, the decrease in Young's modulus and the increase in Poisson's ratio correspond to improve the piezoelectricity. Therefore, it was confirmed by using the pulse echo measurement that oxygen atmosphere firing is an effective tool to improve piezoelectric properties as well as production of pore-free ceramics. Figures 5(a)-(d) show the dependences of the longitudinal and transverse wave velocities, Young's modulus

and Poisson's ratio on the firing position in sagger at a composition of x=0.45 in hard PZT ceramics, respectively. Nos. 1 and 10 in the figure correspond to the top position piled up and the bottom position piled up in sagger (Fig. 6). It became clear that there was fluctuation of the velocities and elastic constants in the case of as-fired (before poling) samples. In addition, the sample of the middle position piled up of No. 5 possesses low wave velocities, low Young's modulus and high Poisson's ratio because of the firing under high lead oxide (PbO) atmosphere. On the other hand, the samples of the top and bottom positions of Nos. 1, 2 and 10 possess high wave velocities, high Young's modulus and low Poisson's ratio because of the firing under low PbO atmosphere due to vaporization of PbO during firing (see Fig. 6). Young's modulus and Poisson's ratio in PZT ceramics of No. 5 could be improved the piezoelectricity (see the session of 4) by high PbO atmosphere firing. However, there is a different tendency to decrease the longitudinal wave velocity [No.5 position in Fig. 5(a)] in comparison with the case of oxygen atmosphere firing [dotted circles at x=0.66, 0.75 in Fig. 4(a)], which also can be improved the elastic constants.

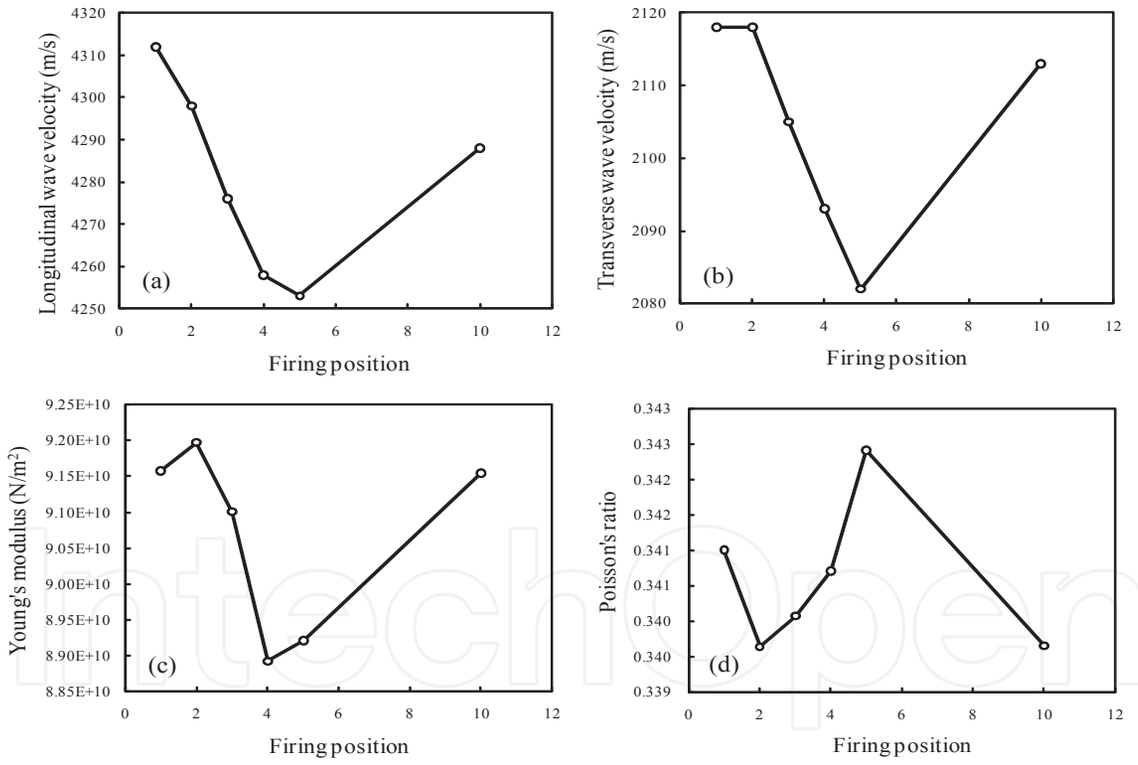

Figure 5. Firing position (Nos. 1 and 10 correspond to ceramic disks of top piled up and bottom piled up in sagger) dependence of (a) longitudinal and (b) transverse wave velocities, (c) Young's modulus and (d) Poisson's ratio in hard PZT ceramics at x=0.45.

We believe that the increase in longitudinal wave velocity [dotted circles at x=0.66, 0.75 in Fig. 4(a)] comes from pore-free microstructure, and further, higher dense and higher Passion's ratio ceramics compared with in the case of normal firing in air atmosphere. Further-

http://dx.doi.org/10.5772/53117

more, it is thought that the fluctuation of as-fired ceramics connected to the fluctuation of ceramics after DC poling.

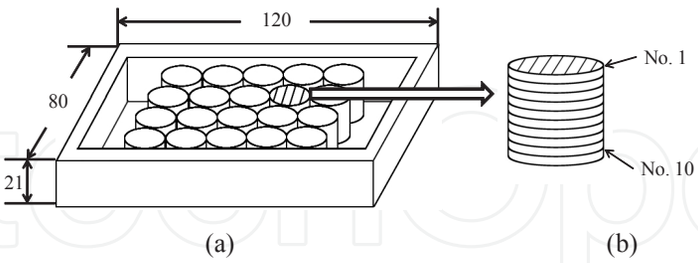

Figure 6. Schematic pictures of (a) PZT green (as-pressed) disks piled up in dense Al_2O_3 sagger (container dimensions: 120 mm length, 80 mm width and 21 mm height) and (b) firing positions (Nos. 1-10) of ceramic green disks (16 mm diameter and 1.2 mm thickness); the ceramic green disk of No. 5 is surrounded with high PbO atmosphere by the other disks piled up, and it is understood that PbO vaporization is easy to occur at the disks of Nos.1, 2 (top) and No.10 (bottom) even through a cover (dense Al_2O_3 ceramic plate) is put on the container while firing [23].

2.3. Young's modulus and Poisson's ratio in lead-free ceramics

Figures 7(a)-(d) show the dependences of the longitudinal and transverse wave velocities, Young's modulus and Poisson's ratio on the composition of lead-free ceramics after poling; the compositions were (1-x)(Na,K,Li,Ba)($Nb_{0.9}Ta_{0.1}$)O_3-xSZ (x=0, 0.02, 0.04, 0.05, 0.06, 0.07), (1-x)NBT-xKBT (x=0.08, 0.11, 0.15, 0.18, 0.21, 0.28), 0.79NBT-0.20KBT-0.01BFT and (1-x)NBT-xBT (x=0.03, 0.07, 0.11), respectively. While the compositions to obtain high electromechanical coupling factor in (Na,K,Li,Ba)($Nb_{0.9}Ta_{0.1}$)O_3-SZ (x=0.05-0.06) and NBT-KBT (x=0.18) [21,22] correspond to the compositions with low Young's modulus and high Poisson's ratio as well as PZT (x=0.48) [3]. Although a MPB existed around x=0.18 in the phase diagram of NBT-KBT [24,25], a MPB did not exist in the phase diagram of (Na,K,Li,Ba)($Nb_{0.9}Ta_{0.1}$)O_3-SZ [20,21]. On the other hand, the compositions with high coupling factor in NBT-BT (x=0.07) [22] possessed low Young's modulus and low Poisson's ratio such as $PbTiO_3$ [6]. In the phase diagram of NBT-BT, it is confirmed that there is a MPB near x=0.07 [26]. Furthermore, there was no significant difference in Young's modulus and Poisson's ratio between as-fired (△) (before poling) and after poling (▲) in (Na,K,Li,Ba)($Nb_{0.9}Ta_{0.1}$)O_3-SZ.

From the above mentioned viewpoint of the study on the elastic constants in lead-free ceramic, it was clarified that there are compositions with high coupling factor in the cases of (1) low Young's modulus and high Poisson's ratio (PZT type) and (2) low Young's modulus and low Poisson's ratio ($PbTiO_3$ type). Namely, it was found that there are two kinds of MPB compositions, (1) and (2) in lead-free ceramics with high coupling factor. Therefore, lead-free ceramic compositions with high piezoelectricity must be primarily focused on to realize the compositions with low Young's modulus such as MPB compositions [27]. Secondarily, the importance to measure Poisson's ratio was understood for the research to recognize the compositions of (1) and (2) in lead-free ceramics with high piezoelectricity.

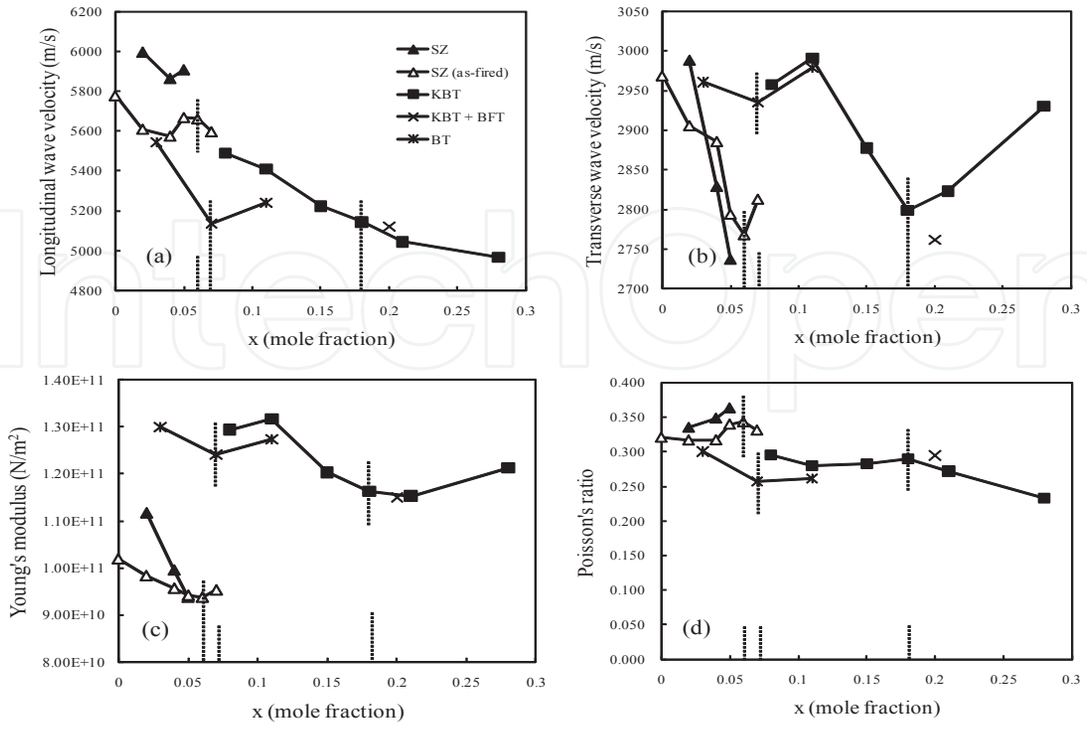

Figure 7. Composition x dependence of (a) longitudinal and (b) transverse wave velocities, (c) Young's modulus and (d) Poisson's ratio in lead-free ceramics of (1-x)(Na,K,Li,Ba)($Nb_{0.9}Ta_{0.1}$)O_3-xSZ (x=0, 0.02, 0.04, 0.05, 0.06, 0.07), (1-x)NBT-xKBT (x=0.08, 0.11, 0.15, 0.18, 0.21, 0.28), 0.79NBT-0.20KBT-0.01BFT and (1-x)NBT-xBT (x=0.03, 0.07, 0.11).

3. Poling field dependence of longitudinal and transverse wave velocities, Young's modulus and Poisson's ratio in piezoelectric ceramics

3.1. DC poling field dependence of elastic constants

As mentioned previously in the session 1, the behavior of ferroelectric domains toward a DC field was investigated on the basis of the DC poling field dependence of dielectric and piezoelectric properties in various types of piezoelectric ceramics and single crystals. In addition, we have developed a method to evaluate elastic constants, such as Young's modulus and Passion's ratio, by measuring longitudinal and transverse wave velocities using an ultrasonic thickness gauge with high-frequency pulse oscillation in comparison with a conventional method as described in the session 2. The acoustic wave velocities can be measured by this method in the cases of ceramics and single crystals despite the strength of the DC poling field, including as-fired ceramics and as-grown single crystals.

Therefore, in order to clarify the relationships between elastic constants and electrical properties vs DC poling fields, we studied the poling field dependence of acoustic wave velocities and dielectric and piezoelectric properties in ceramics. Here, we report the relationships

http://dx.doi.org/10.5772/53117

between DC poling fields, acoustic wave velocities, Young's modulus, and Passion's ratio to realize a high piezoelectricity, especially in lead-free ceramics.

The piezoelectric ceramic compositions measured were as follows: $0.05Pb(Sn_{0.5}Sb_{0.5})O_3$-$(0.95\text{-}x)PbTiO_3$-$xPbZrO_3$ (x=0.33, 0.45, 0.66) with (hard PZT) and without 0.4 wt% MnO_2 (soft PZT); $0.90PbTiO_3$-$0.10La_{2/3}TiO_3$(PLT) and $0.975PbTiO_3$-$0.025La_{2/3}TiO_3$(PT); (1-x)$(Na,K,Li,Ba)(Nb_{0.9}Ta_{0.1})$ O_3-$xSrZrO_3$(SZ) (x=0.00, 0.05, 0.07); (1-x)$(Na_{0.5}Bi_{0.5})TiO_3$(NBT)-$x(K_{0.5}Bi_{0.5})TiO_3$(KBT) (x=0.08, 0.18) and 0.79NBT-0.20KBT-$0.01Bi(Fe_{0.5}Ti_{10.5})O_3$(BFT) (x= 0.20); and (1-x)NBT-$xBaTiO_3$(BT) (x=0.03, 0.07, 0.11).

DC poling was conducted for 30 min at the most suitable poling temperature depending on the Curie points of the ceramic materials when the poling field (E) was varied from 0→ +0.25→+0.5→+0.75→ +1.0→ --- $+E_{max}$→0→$-E_{max}$→0 to $+E_{max}$ kV/mm. $\pm E_{max}$ depended on the coercive fields of the piezoelectric ceramics. After each poling process, the dielectric and piezoelectric properties were measured at room temperature using an LCR meter (HP4263A), a precision impedance analyzer (Agilent 4294A), and a piezo d_{33} meter (Academia Sinica ZJ-3D). Furthermore, the acoustic wave velocities were measured using an ultrasonic precision thickness gauge (Olympus 35DL), which has PZT transducers with 30 MHz for longitudinal-wave generation and 20 MHz for transverse-wave generation. The acoustic wave velocities were evaluated on the basis of the propagation time between the second-pulse echoes in the thickness of ceramic disks parallel to the poling field with dimensions of 14 mm diameter and 0.5-1.5 mm thickness. The sample thickness was measured using a precision micrometer (Mitutoyo MDE-25PJ). Moreover, Young's modulus in the thickness direction of ceramic disks (Y_{33}^E) and Passion's ratio (σ) were calculated on the basis of the longitudinal (V_L) and transverse (V_S) wave velocities as shown in the following equations:

$$Y_{33}^E = 3\varrho V_S^2 \frac{V_L^2 - \frac{4}{3}V_S^2}{V_L^2 - V_S^2} \text{ and } \sigma = \frac{1}{2}\left\{1 - \frac{1}{\left(\frac{V_L}{V_S}\right)^2 - 1}\right\},$$

where ϱ is the density of ceramic disks.

3.2. Poling field dependence in PZT ceramics

Figures 8-10 show the poling field dependence of longitudinal (V_L) and transverse (V_S) wave velocities, Young's modulus (Y_{33}^E), and Passion's ratio (σ) in $0.05Pb(Sn_{0.5}Sb_{0.5})O_3$-$(0.95\text{-}x)PbTiO_3$-$xPbZrO_3$ (x=0.33, 0.45, 0.66) with (hard PZT) and without 0.4 wt% MnO_2 (soft PZT) ceramics at a poling temperature (T_P) of 80 °C (hard PZT in Fig. 8 and soft PZT in Fig. 9), $0.90PbTiO_3$-$0.10La_{2/3}TiO_3$ (abbreviate to PLT/T_p=80 °C) and $0.975PbTiO_3$-$0.025La_{2/3}TiO_3$ (abbreviate to PLT /T_p=200 °C) ceramics (Fig. 10), respectively. While the poling field dependence of V_L has almost same tendency in spite of hard and soft PZT, the one of V_S at x=0.45, which corresponds to MPB, abruptly decreases in the both cases of hard and soft PZT (Figs. 8, 9). Since the highest coupling factor in PZT is obtained at the MPB (x=0.45), the origin of the highest piezoelectricity is due to the decrease in V_S with increasing the domain alignment by DC poling field. Furthermore, the lowest Y_{33}^E and the highest σ are realized at the MPB. The change in V_L, V_S, Y_{33}^E and σ vs E of soft PZT is smaller than the one of hard PZT because of the softness of the materials. As mentioned details to the next session 3.3, it was

indicated that minimum V_L, σ and maximum V_S, Y_{33}^E were obtained at the domain clamping such as the domain alignment canceled each other (↑↓), at which the lowest piezoelectricity is realized. On the other hand, the values of V_L, V_S, Y_{33}^E and σ vs E in PT are smaller than the ones of PLT. Moreover, at the domain clamping fields, minimum V_L, σ, Y_{33}^E and maximum V_S were obtained in both the PLT and PT. The reason of minimum Y_{33}^E at the DC field of the domain clamping will be discuss in the next session. In addition, the change in Y_{33}^E of PLT and PT while applying ±E is smaller than the one of PZT, and higher Y_{33}^E and lower σ appear in comparison with the ones of PZT, because these come from the hardness of PLT and PT ceramics.

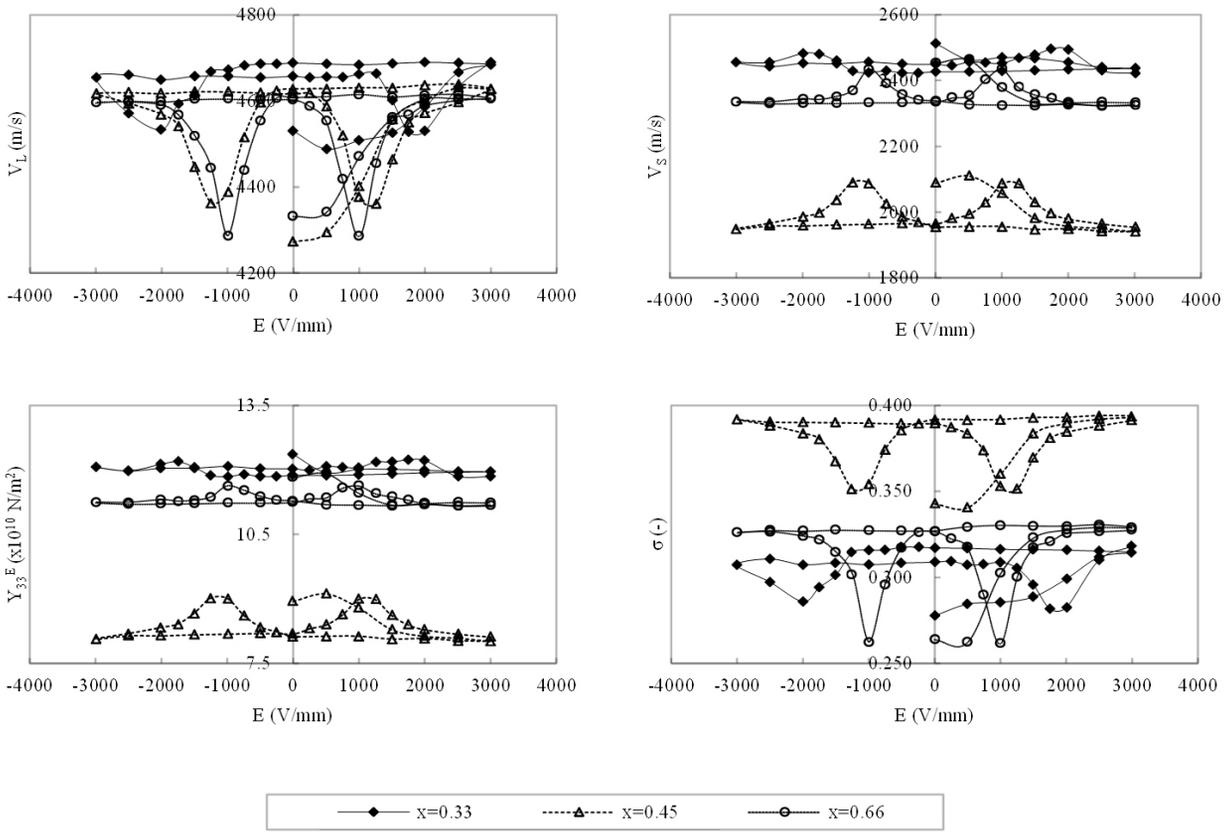

Figure 8. Poling field dependence of longitudinal (V_L) and transverse (V_S) wave velocities, Young's modulus (Y_{33}^E), and Poisson's ratio (σ) in $0.05Pb(Sn_{0.5}Sb_{0.5})O_3$-$(0.95\text{-}x)PbTiO_3$-$xPbZrO_3$ (x=0.33, 0.45, 0.66) with 0.4 wt% MnO_2 (hard PZT) ceramics.

http://dx.doi.org/10.5772/53117

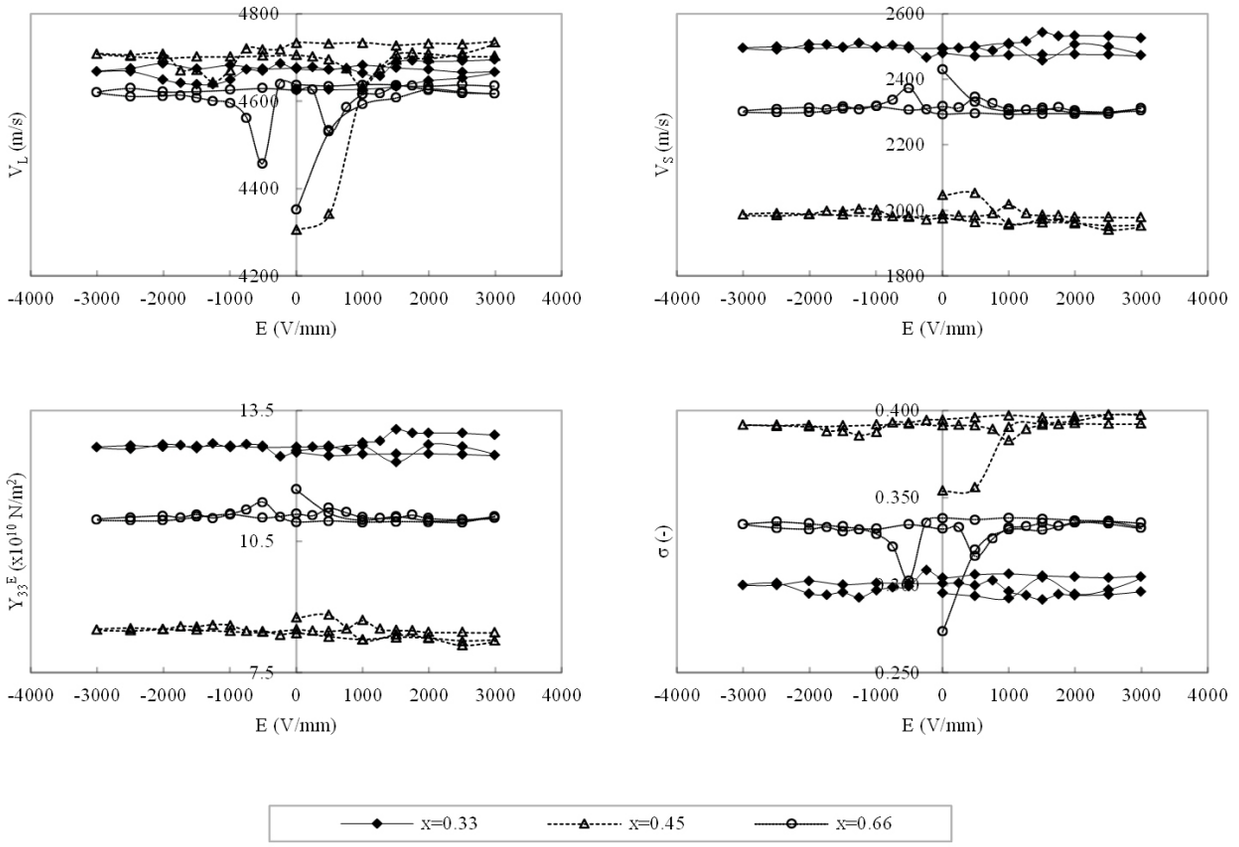

Figure 9. Poling field dependence of longitudinal (V_L) and transverse (V_S) wave velocities, Young's modulus (Y_{33}^E), and Poisson's ratio (σ) in $0.05Pb(Sn_{0.5}Sb_{0.5})O_3$-$(0.95-x)PbTiO_3$-$xPbZrO_3$ (x=0.33, 0.45, 0.66) without 0.4 wt% MnO_2 (soft PZT) ceramics.

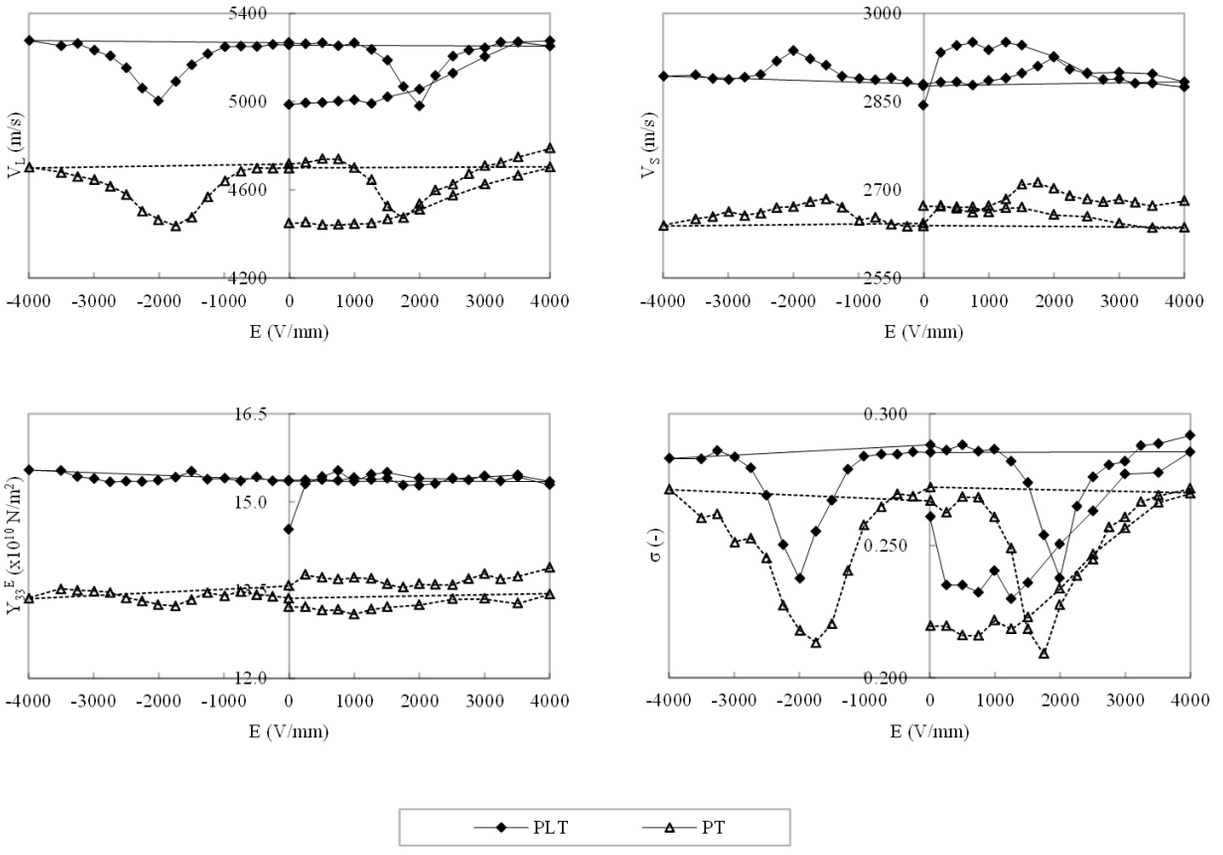

Figure 10. Poling field dependence of longitudinal (V_L) and transverse (V_S) wave velocities, Young's modulus (Y_{33}^E), and Poisson's ratio (σ) in 0.90$PbTiO_3$-0.10$La_{2/3}TiO_3$ (PLT) and 0.975$PbTiO_3$-0.025$La_{2/3}TiO_3$ (PLT) ceramics.

3.3. Poling field dependence in lead-free ceramics

Figures 11-13 show the poling field dependence of longitudinal (V_L) and transverse (V_S) wave velocities, Young's modulus (Y_{33}^E), and Passion's ratio (σ) in (1-x)(Na,K,Li,Ba)($Nb_{0.9}Ta_{0.1}$)O_3-x$SrZrO_3$(SZ) (x=0.00, 0.05, 0.07) ceramics at a poling temperature (T_P) of 150 °C (Fig. 11), in (1-x)($Na_{0.5}Bi_{0.5}$)TiO_3(NBT)-x($K_{0.5}Bi_{0.5}$)TiO_3(KBT) (x=0.08, 0.18/ T_p=70 °C) and 0.79NBT-0.20KBT-0.01Bi($Fe_{0.5}Ti_{10.5}$)O_3(BFT) (x=0.20/ T_p=70 °C) ceramics (Fig. 12), and in (1-x)NBT-x$BaTiO_3$(BT) (x=0.03, 0.07, 0.11/ T_p=70 °C) ceramics (Fig. 13), respectively. With the enhancement of domain alignment with an increase in poling field from E=0 to $+E_{max}$, V_L increased and V_S decreased independently of the ceramic composition. From the composition dependence of Y_{33}^E and σ, high piezoelectricity [high planar coupling factor (k_p)] compositions show lower Y_{33}^E and higher σ values at 0.95(Na,K,Li,Ba)($Nb_{0.9}Ta_{0.1}$)O_3-0.05SZ (k_p=46%) (Fig. 11) and 0.82NBT-0.18KBT (k_p=27%) (Fig. 12) as well as the ones at 0.05Pb($Sn_{0.5}Sb_{0.5}$)O_3-0.47$PbTiO_3$-0.48$PbZrO_3$ (k_p=65% in soft ceramics and k_p=52% in hard ceramics) than the other compositions. Although morphotropic phase boundaries (MPBs) were observed in the NBT-KBT [24,25] and PZT [3,23,28] ceramics, there was no evidence of the existence of MPBs in the (Na,K,Li,Ba)($Nb_{0.9}Ta_{0.1}$)O_3-SZ ceramics [20,21]. The effects of 0.01BFT modification in NBT-KBT on Y_{33}^E and σ were as follows: the composition of

0.79NBT-0.20KBT-0.01BFT (k_p=22%; x=0.20 in Fig. 12) showed the highest piezoelectric d_{33} constant of 150 pC/N in NBT-KBT and higher Y_{33}^E and lower σ values than that of 0.82NBT-0.18KBT (k_p=27%; x=0.18 in Fig. 12) because the relative dielectric constant increased from 800 (0.82NBT-0.18KBT) to 1250 (0.79NBT-0.20KBT-0.01BFT) [22]. Moreover, a high-coupling-factor composition at 0.93NBT-0.07BT (k_p=16%) existed in a MPB [26] with a low Y_{33}^E (Fig. 13).

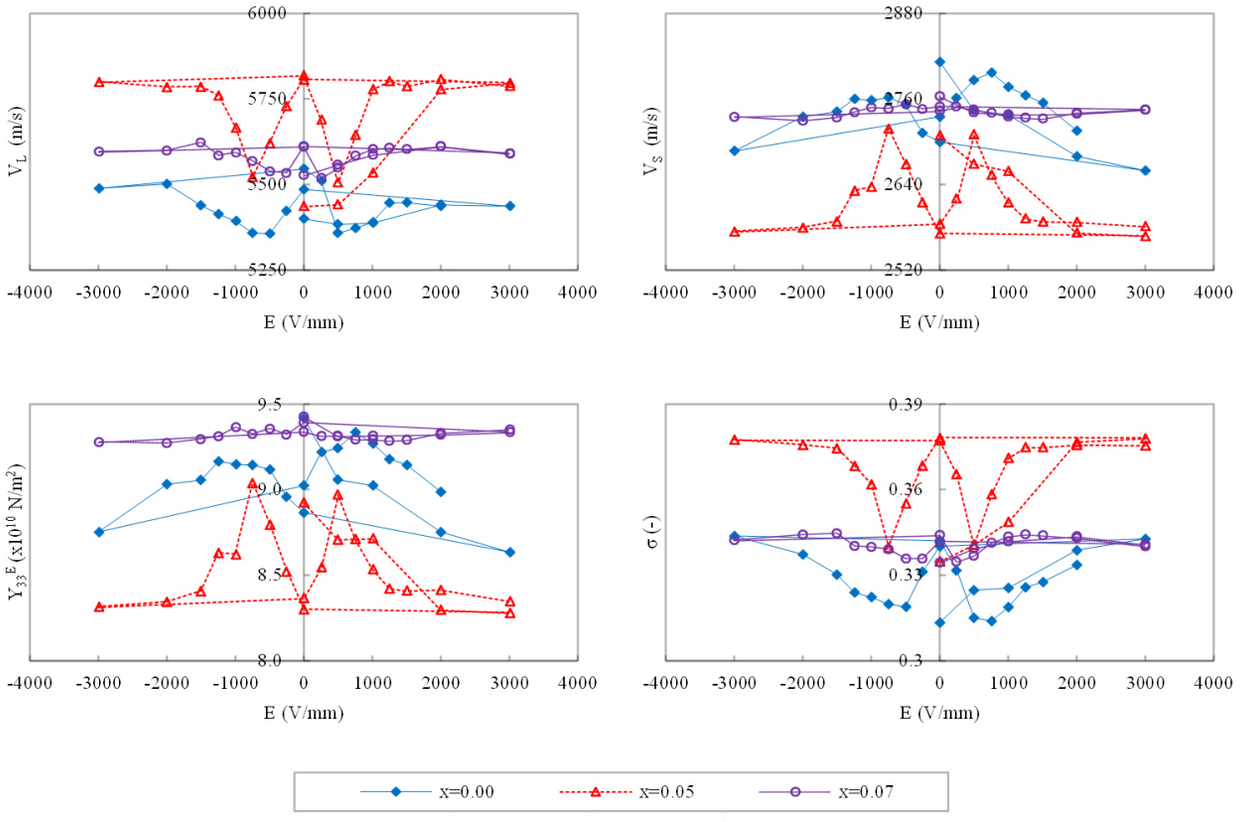

Figure 11. Poling field dependence of longitudinal (V_L) and transverse (V_S) wave velocities, Young's modulus (Y_{33}^E), and Poisson's ratio (σ) in (1-x)(Na,K,Li,Ba)($Nb_{0.9}Ta_{0.1}$)O_3-x$SrZrO_3$ (x=0.00, 0.05, 0.07) ceramics.

Basically, research on piezoelectric ceramics with high planar coupling factors, especially in lead-free ceramics, has been focused on determining the MPB composition because many different polarization axes are generated in MPB.

Through our study on acoustic wave measurement, it was found that there was an important factor for obtaining a high piezoelectricity regarding Y_{33}^E and σ; lower Y_{33}^E and higher σ

values in the cases of PZT, alkali bismuth titanate [NBT-KBT], and alkali bismuth barium titanate [NBT-BT] with MPB, and in the case of alkali niobate [(Na,K,Li,Ba)($Nb_{0.9}Ta_{0.1}$)O_3-SZ] without MPB. Therefore, as mentioned later, we need a new concept in addition to conventional research on MPB compositions for developing piezoelectric ceramics with high coupling factors.

The DC poling fields under domain clamping (E_d) can be estimated on the basis of E values to realize the minimum V_L and maximum V_S in Figs. 11-13. Although the maximum Y_{33}^E and minimum σ were obtained at E_d, which corresponds to the E of the minimum coupling factor in (Na,K,Li,Ba)($Nb_{0.9}Ta_{0.1}$)O_3-SZ (Fig. 11), NBT-KBT, and 0.79NBT-0.20KBT-0.01BFT (Fig. 12), the minimum Y_{33}^E and minimum σ were obtained at E_d in NBT-BT (Fig. 13). It was clarified that the minimum Y_{33}^E in NBT-BT was realized in the cases of $\Delta V_S/\Delta V_L<1/4$ at E_d, where ΔV_S and ΔV_L denote the variations in V_S and V_L at E_d, respectively. This may be due to the poor domain alignment (lower Poisson's ratio) perpendicular to the poling field (radial direction in disk ceramics) in comparison with the domain alignment parallel to the poling field (thickness direction in disk ceramic). Furthermore, the increase in coupling factor corresponds to the increase in σ at all compositions including lead-containing and lead-free ceramic compositions.

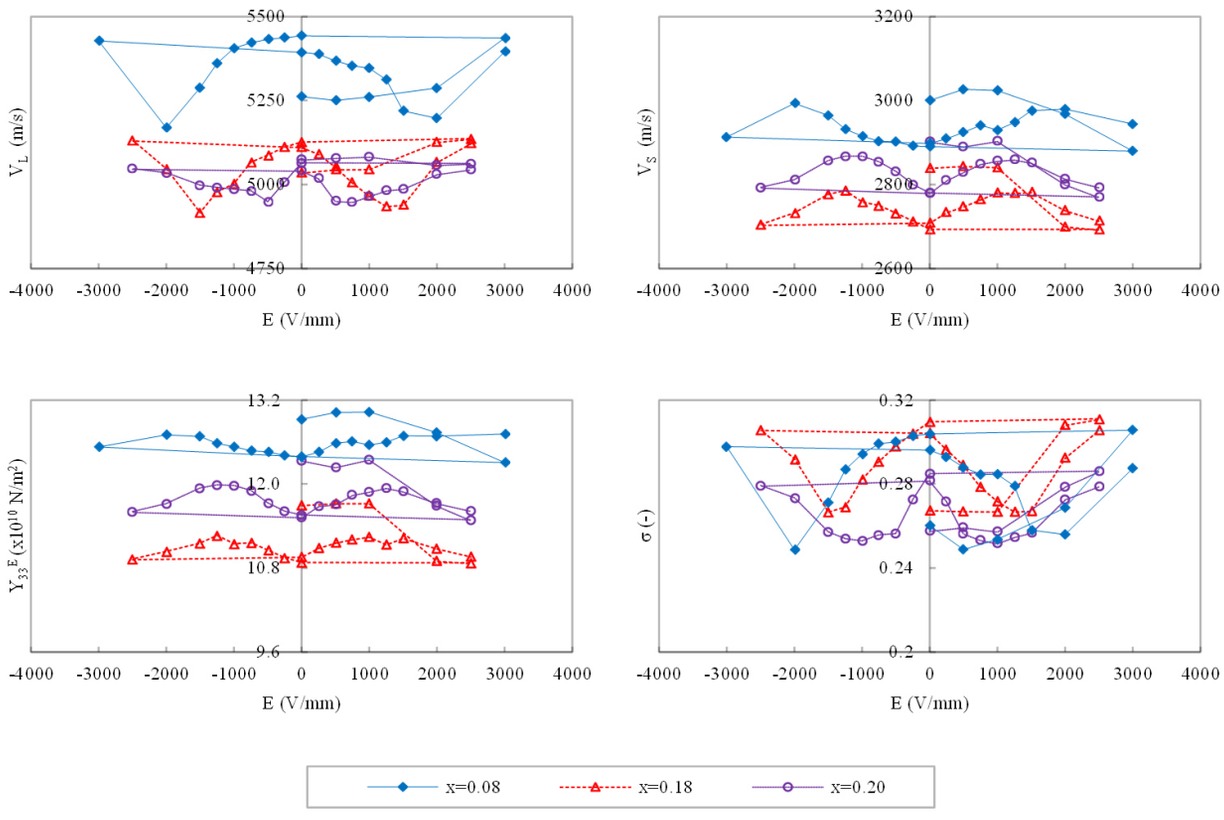

Figure 12. Poling field dependence of longitudinal (V_L) and transverse (V_S) wave velocities, Young's modulus (Y_{33}^E), and Poisson's ratio (σ) in (1-x)NBT-xKBT (x=0.08, 0.18) and 0.79NBT-0.2KBT-0.01BFT (x=0.20) ceramics.

http://dx.doi.org/10.5772/53117

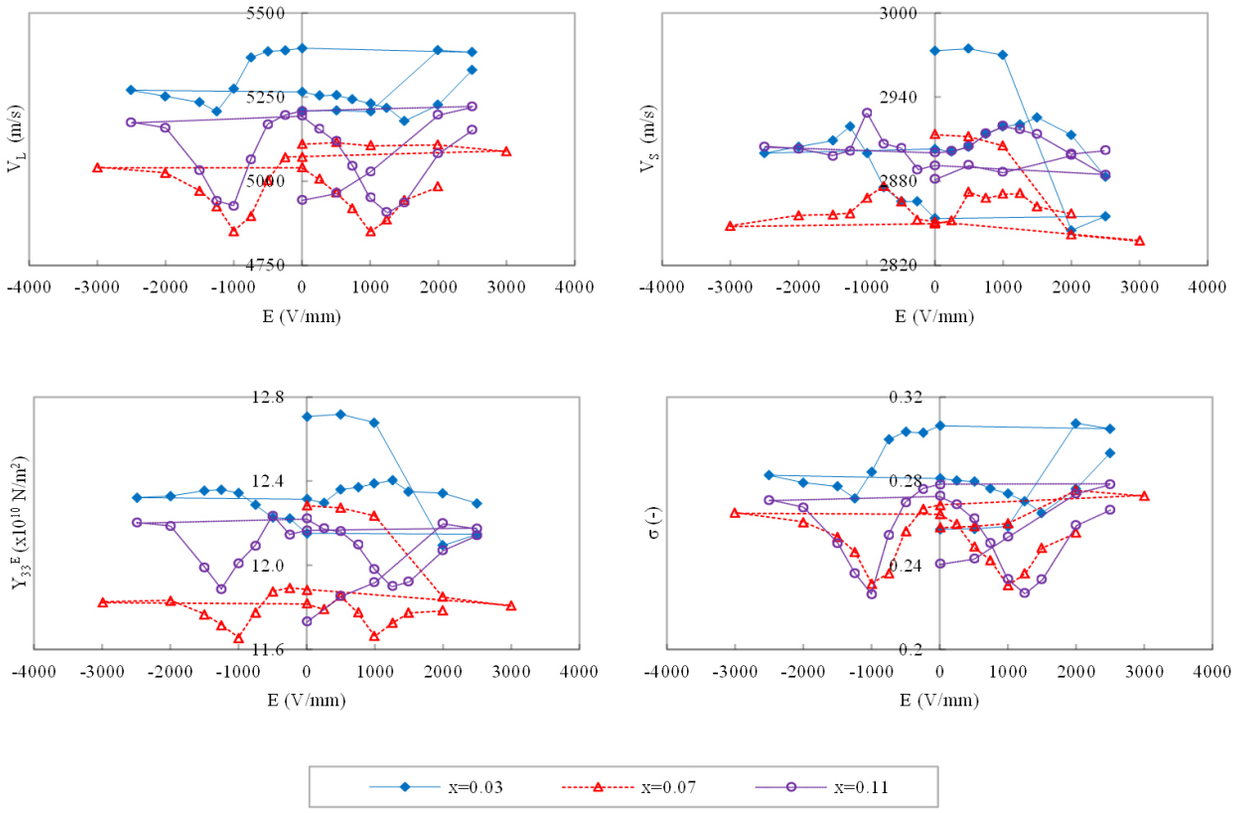

Figure 13. Poling field dependence of longitudinal (V_L) and transverse (V_S) wave velocities, Young's modulus (Y_{33}^E), and Poisson's ratio (σ) in (1-x)NBT-xBT (x=0.03, 0.07, 0.11) ceramics.

4. Materials road maps in piezoelectric ceramics on elastic constants

Figure 14 shows the relationships between longitudinal (V_L) and transverse (V_S) wave velocities, Young's modulus (Y_{33}^E), and Passion's (σ) ratio vs planar coupling factors (k_p) in (1-x)(Na,K,Li,Ba)($Nb_{0.9}Ta_{0.1}$)O_3-xSZ (abbreviated to "SZ"), (1-x)NBT-xKBT ("KBT"), 0.79NBT-0.20KBT-0.01BFT ("KBT"), and (1-x)NBT-xBT ("BT") lead-free ceramics compared with 0.05Pb($Sn_{0.5}Sb_{0.5}$)O_3-(0.95-x)$PbTiO_3$-x$PbZrO_3$ ceramics with ("hard PZT") and without 0.4 wt % MnO_2 ("soft PZT"), and with 0.90$PbTiO_3$-0.10$La_{2/3}TiO_3$ ("PLT") and 0.975$PbTiO_3$-0.025 $La_{2/3}TiO_3$ ("PT") lead-containing ceramics after full DC poling. Although the V_L values of the PZT ceramics were almost constant at approximately 4,600-4,800 m/s independently of the composition x, their V_S values linearly decreased from 2,500 to 1,600 m/s with increasing k_p from 20 to 65% (solid lines). In addition, the V_L and V_S values of the PZT ceramics were smaller than those of the lead-free ceramics (V_L=5,000-5,800 m/s and V_S=2,600-3,000 m/s; dashed and dotted lines). Although the V_L values of the PT ceramics were almost the same (4,800 m/s) as those of the PZT ceramics, the V_S values of the PT ceramics were approximately 2,700 m/s. On the other hand, the V_L values of the SZ ceramics were relatively high (5,500-5,800 m/s); furthermore, the V_S values of the SZ ceramics also increased (2,600-2,700 m/s) and linearly decreased with increasing k_p from 25 to 50% (dashed lines), the behavior of

which was almost the same as that of the V_S values of the PZT ceramics. The V_L values of the KBT, BT, and PLT ceramics (5,000-5,400 m/s) were between those of the PZT, PT, and SZ ceramics. However, the V_S values of the KBT, BT, and PLT ceramics (2,800-3,000 m/s) were the highest. Therefore, it was possible to divide V_L and V_S into three material groups, namely, PZT and PT/ KBT, BT (alkali bismuth titanate), and PLT/ SZ (alkali niobate). In addition, k_p lineally increased from 4 to 65% with decreasing Y_{33}^E from 15×10^{10} to 6×10^{10} N/m^2 and lineally increased with increasing σ from 0.25 to 0.43. It was clarified that higher k_p values can be realized at lower Y_{33}^E and higher σ values.

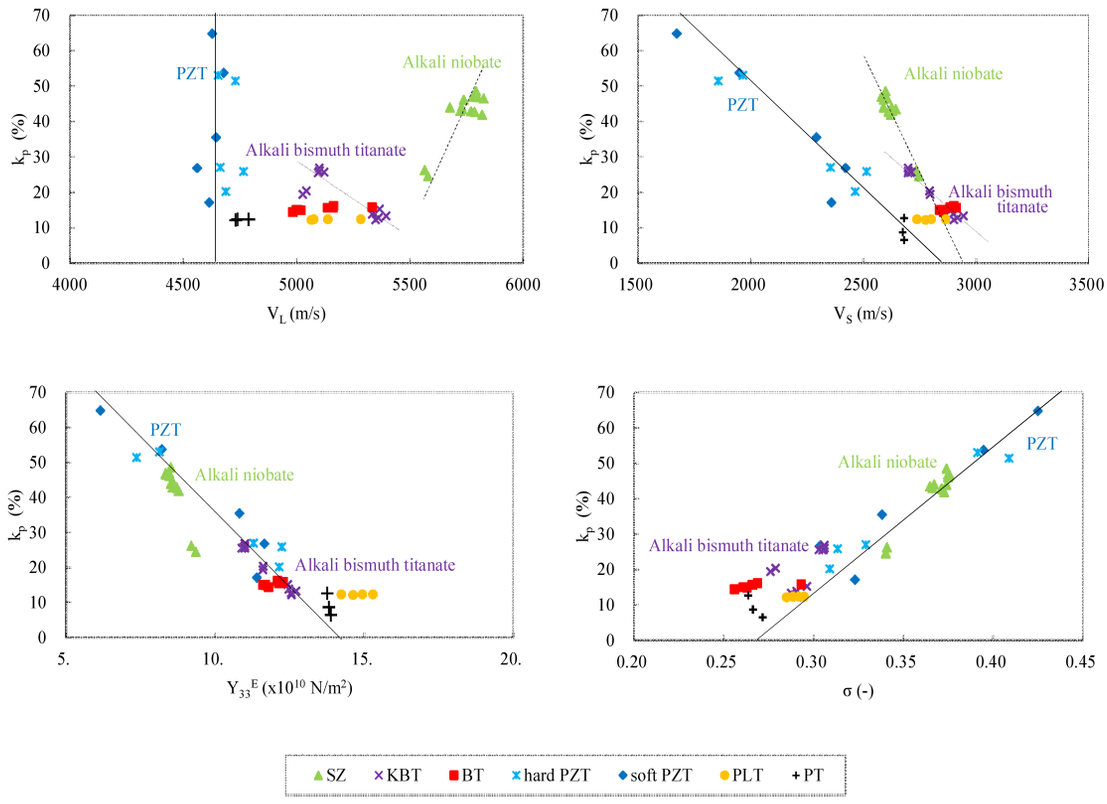

Figure 14. Relationships between longitudinal (V_L) and transverse (V_S) wave velocities, Young's modulus (Y_{33}^E), and Passion ratio (σ) vs planar coupling factors (k_p) in (1-x)(Na,K,Li,Ba) $(Nb_{0.9}Ta_{0.1})O_3$-xSZ (abbreviated to "SZ"), (1-x)NBT-xKBT ("KBT"), 0.79NBT-0.20KBT-0.01BFT ("KBT"), and (1-x)NBT-xBT ("BT") lead-free ceramics compared with $0.05Pb(Sn_{0.5}Sb_{0.5})O_3$-(0.95-x) $PbTiO_3$-x$PbZrO_3$ ceramics with ("hard PZT") and without 0.4 wt% MnO_2 ("soft PZT"), and with 0.90$PbTiO_3$-0.10$La_{2/3}TiO_3$ ("PLT") and 0.975$PbTiO_3$-0.025$La_{2/3}TiO_3$ ("PT") lead-containing ceramics after full DC poling.

http://dx.doi.org/10.5772/53117

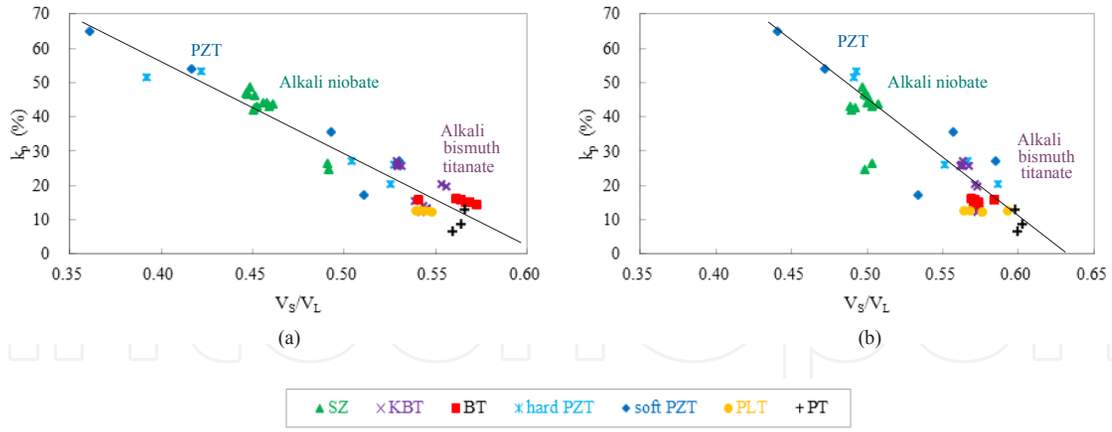

Figure 15. Ratio of longitudinal wave velocity (V_L) to transverse wave velocity (V_S): V_S/V_L vs k_p in lead-containing ceramics [$0.05Pb(Sn_{0.5}Sb_{0.5})O_3$-$(0.95-x)PbTiO_3$-$xPbZrO_3$ with ("hard PZT") and without 0.4 wt% MnO_2 ("soft PZT"), $0.90PbTiO_3$-$0.10La_{2/3}TiO_3$ ("PLT"), and $0.975PbTiO_3$-$0.025La_{2/3}TiO_3$ ("PT")] and in lead-free ceramics [$(1-x)(Na,K,Li,Ba)(Nb_{0.9}Ta_{0.1})O_3$-xSZ (abbreviated to "SZ"), (1-x)NBT-xKBT ("KBT"), 0.79NBT-0.20KBT-0.01BFT ("KBT"), and (1-x)NBT-xBT ("BT")] (a) after and (b) before full DC poling.

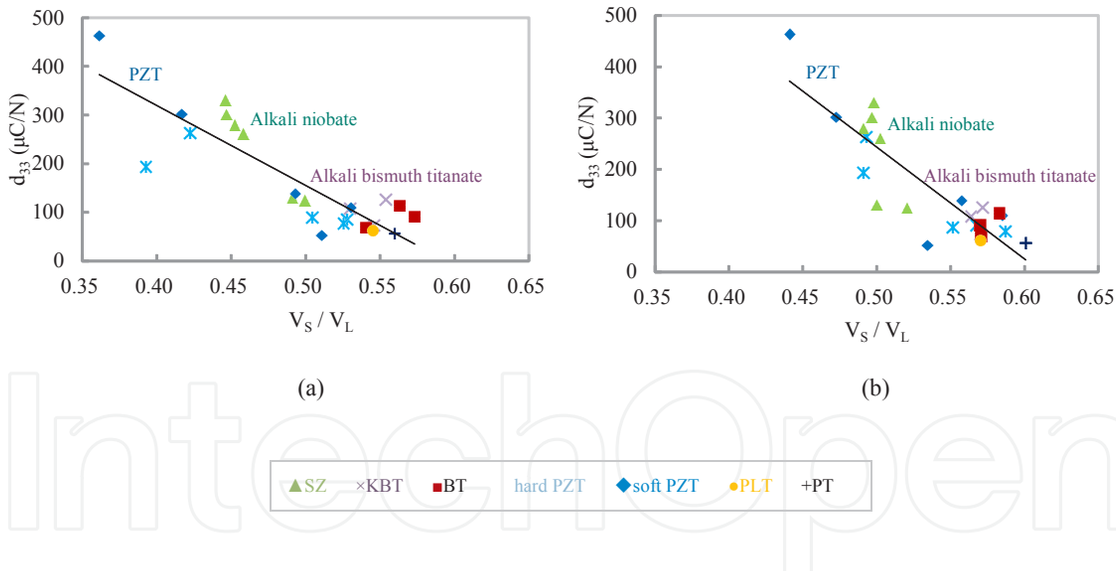

Figure 16. Ratio of longitudinal wave velocity (V_L) to transverse wave velocity (V_S): V_S/V_L vs piezoelectric strain constant d_{33} in lead-containing ceramics ["hard PZT", "soft PZT", "PLT" and "PT"] and in lead-free ceramics ["SZ", "KBT" and "BT"] (a) after and (b) before full DC poling.

Figures 15 and 16 show the ratio of V_L to V_S vs k_p and V_S/V_L vs piezoelectric strain constant d_{33} in lead-containing and lead-free ceramics (a) after and (b) before full DC poling, respectively. There are linear relationships between V_S/V_L vs k_p and d_{33} in spite of DC poling treatment; with decreasing V_S/V_L from 0.58 to 0.36, k_p increased from 4 to 65% (correlation

coefficient r=-0.96 after poling and r=-0.89 before poling) and d_{33} also increased from 52 to 463 μC/N (r=-0.87 in both after and before poling). This means that it is possible to estimate the degree of piezoelectricity (the values of k_p and d_{33}) from V_S/V_L, even though the ceramics were without DC poling (as-fired).

Furthermore, we can mention that it is significant to evaluate the both values of k_p and d_{33}, which are not directly corresponding to each other because of $d=k(\varepsilon \cdot s)^{1/2}$ (d: piezoelectric strain constant, k: coupling factor, ε: dielectric constant, s: compliance). Therefore, our developed method for acoustic wave velocity measurement, especially V_S/V_L, is useful for materials research on piezoelectric ceramics including lead-free ceramics with higher coupling factor and higher piezoelectric strain constant d_{33} in the cases of as-fired [Figs. 15(b) and 16(b)] as well as DC fully polarized [Figs. 15(a) and 16(a)] ceramics.

This session was described the road maps in piezoelectric ceramics between longitudinal and transvers wave velocity, Young's modulus and Poisson's ratio to research and develop new piezoelectric ceramic materials, especially lead-free ceramics with high piezoelectricity.

5. Conclusions

Longitudinal and transverse wave velocities of PZT, lead titanate and lead-free ceramics were measured by an ultrasonic precision thickness gauge with high-frequency pulse oscillation to calculate elastic constants such as Young's modulus and Poisson's ratio. The dependences of compositions and manufacturing processes of the ceramics on the elastic constants were clarified in PZT ceramics. Moreover, while the compositions around MPB in lead-free ceramics were investigated by this method, it was found significant relationships between Young's modulus and Poisson's ratio in lead-free ceramics with high piezoelectricity. The DC poling field dependence of the longitudinal and transverse wave velocities of PZT, lead titanate, and lead-free ceramics was also investigated by this method. The effect of the poling field on domain alignment, such as in the cases of full DC poling and domain clamping, could be explained by the relationships between acoustic wave velocities, Young's modulus, and Poisson's ratio vs poling field. The directions of the research and development of piezoelectric ceramics including lead-free ceramics with high coupling factors could be proposed on the basis of the findings of this study.

Acknowledgments

This work was partially supported by a Grant-in-Aid for Scientific Research C (No. 21560340) and a Grant of Strategic Research Foundation Grant-aided Project for Private Universities 2010-2014 (No. S1001032) from the Ministry of Education, Culture, Sports, Science and Technology, Japan (MEXT).

Author details

Toshio Ogawa

Department of Electrical and Electronic Engineering, Shizuoka Institute of Science and Technology, Toyosawa, Fukuroi, Shizuoka, Japan

References

[1] Ogawa T, Yamada A, Chung YK, Chun DI. Effect of Domain Structures on Electrical Properties in Tetragonal PZT Ceramics. J. Korean Phys. Soc. 1998;32: S724-S726.

[2] Ogawa T, Nakamura K. Poling Field Dependence of Ferroelectric Properties and Crystal Orientation in Rhombohedral Lead Zirconate Titanate Ceramics. Jpn. J. Appl. Phys. 1998;37: 5241-5245.

[3] Ogawa T, Nakamura K. Effect of Domain Switching and Rotation on Dielectric and Piezoelectric Properties in Lead Zirconate Titanate Ceramics. Jpn. J. Appl. Phys. 1999;38: 5465-5469.

[4] Ogawa T. Domain Switching and Rotation in Lead Zirconate Titanate Ceramics by Poling Fields. Ferroelectrics 2000;240: 75-82.

[5] Ogawa T. Domain Structure of Ferroelectric Ceramics. Ceram. Int. 2000;25: 383-390.

[6] Ogawa T. Poling Field Dependence of Crystal Orientation and Ferroelectric Properties in Lead Titanate Ceramics. Jpn. J. Appl. Phys. 2000;39: 5538-5541.

[7] Ogawa T. Poling Field Dependence of Ferroelectric Properties in Barium Titanate Ceramics. Jpn. J. Appl. Phys. 2001;40: 5630-5633.

[8] Ogawa T. Poling Field Dependence of Ferroelectric Properties in Piezoelectric Ceramics and Single Crystal. Ferroelectrics 2002;273: 371-376.

[9] Kato R, Ogawa T. Chemical Composition Dependence of Giant Piezoelectricity on k_{31} Mode in $Pb(Mg_{1/3}Nb_{2/3})O_3$–$PbTiO_3$ Single Crystals. Jpn. J. Appl. Phys. 2006; 45: 7418-7421.

[10] Ogawa T, Yamauchi Y, Numamoto Y, Matsushita M, Tachi Y. Giant Electromechanical Coupling Factor of k_{31} Mode and Piezoelectric d_{31} Constant in $Pb[(Zn_{1/3}Nb_{2/3})_{0.91}Ti_{0.09}]O_3$ Piezoelectric Single Crystal. Jpn. J. Appl. Phys. 2002;41: L55-L57.

[11] Ogawa T. Giant k_{31} Relaxor Single-Crystal Plate and Their Applications. In: Lallart M. (ed.) Ferroelectrics-Applications. Rijeka: InTech; 2011. P.3-34.

[12] Ogawa T, Numamoto Y. Origin of Giant Electromechanical Coupling Factor of k_{31} Mode and Piezoelectric d_{31} Constant in $Pb[(Zn_{1/3}Nb_{2/3})_{0.91}Ti_{0.09}]O_3$ Single Crystal. Jpn. J. Appl. Phys. 2002;41: 7108-7112.

[13] Technical catalogues 2004 for piezoelectric materials of TDK Corporation, Murata Manufacturing Co., Ltd., Fuji Ceramics Corporation, NEC Tokin Corporation, etc.

[14] Kadota M, Saito Y, Yoshida T, Ozeki H, Yamaguchi T, Hasegawa M, Sato H. EMAS-6100, Standard of Electronic Materials Manufacturers Association of Japan. Tokyo: Piezoelectric Ceramics Technical Committee; 1993 [in Japanese].

[15] Bechmann R. IRE Standards on Piezoelectric Crystals. Proc. IRE, 1958.

[16] Shibayama K. Danseiha Soshi Gijyutsu Handbook (Technical Handbook of Acoustic Wave Devices). Tokyo: Ohmsha; 1991 [in Japanese].

[17] Mason WP. Physical Acoustics I, Part A. New York: Academic Press; 1964.

[18] Takagi K. Cyouonpa Binran (Ultrasonic Handbook). Tokyo: Maruzen; 1999 [in Japanese].

[19] Negishi K, Takagi K. Cyouonpa Gijutsu (Ultrasonic Technology). Tokyo: Univ. of Tokyo Press; 1984 [in Japanese].

[20] Furukawa M, Tsukada T, Tanaka D, Sakamoto N. Alkaline Niobate-based Lead-Free Piezoelectric Ceramics. Proc. 24th Int. Japan-Korea Semin. Ceramics, 2007.

[21] Ogawa T, Furukawa M, Tsukada T. Poling Field Dependence of Piezoelectric Properties and Hysteresis Loops of Polarization versus Electric Field in Alkali Niobate Ceramics. Jpn. J. Appl. Phys. 2009;48, 709KD07-1-5.

[22] Ogawa T, Nishina T, Furukawa M, Tsukada T. Poling Field Dependence of Ferroelectric Properties in Alkali Bismuth Titanate Lead-Free Ceramics. Jpn. J. Appl. Phys. 2010; 49: 09MD07-1-4.

[23] Ogawa T. Highly Functional and High-Performance Piezoelectric Ceramics. Ceramic Bulletin 1991;70: 1042-1049.

[24] Zhao W, Zhou H, Yan Y, Liu D. Morphotropic Phase Boundary Study of the BNT-BKT Lead-Free Piezoelectric Ceramics. Key Eng. Mater. 2008;368-372: 1908-1910.

[25] Yang Z, Liu B, Wei L, Hou Y. Structure and Electrical Properties of $(1-x)Bi_{0.5}Na_{0.5}TiO_3$-$xBi_{0.5}K_{0.5}TiO_3$ Ceramics near Morphotropic Phase Boundary. Mater. Res. Bull. 2008;43: 81-89.

[26] Dai Y, Pan J,Zhang X. Composition Range of Morphotropic Phase Boundary and Electrical Properties of NBT-BT System. Key Eng. Mater. 2007; 336-338: 206-209.

[27] Saito Y, Takao H, Tani T, Nonoyama T, Takatori K, Homma T, Nagaya T, Nakamura M. Lead-Free Piezoceramics. Nature 2004;432: 84-87.

[28] Jaffe B, Cook WR, and Jaffe H. Piezoelectric Ceramics. New York: Academic Press; 1971.

IntechOpen

IntechOpen